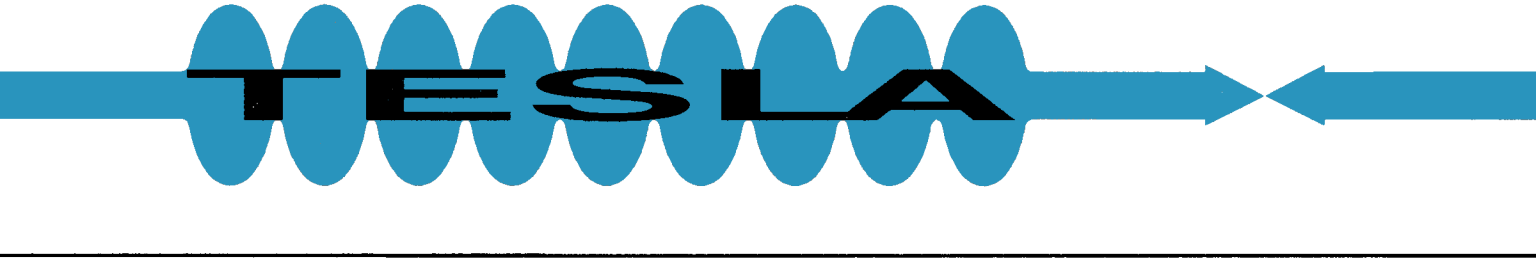

TESLA - COLLABORATION

Energy Propagation through the TESLA Channel: The Regime of the First Waveguide Mode

H.-W. Glock, M. Kurz, P. Hülsmann, W.F.O. Müller, U. Niermann, C. Peschke, H. Klein

Johann Wolfgang Goethe Universität Frankfurt/Main

DESY Print April 1995, TESLA 95-07

TESLA Reports are available from:

Deutsches Elektronen-Synchrotron DESY
MHF-SL Group
Katrin Lando
Notkestraße 85
Postfach
22603 Hamburg
FRG

Phone: (0049/40) 8998 3339
Fax: (0049/40) 8994 4302
e-mail: LANDO@LANDO.DESY.DE
Telex: 2 15 124 desy d

Energy Propagation through the TESLA Channel: The Regime of the First Waveguide Mode

H.-W. Glock, M. Kurz, P. Hülsmann, W.F.O. Müller, U. Niermann, C.Peschke, H. Klein

Institut für Angewandte Physik
der Johann Wolfgang Goethe - Universität Frankfurt am Main

Robert Mayer Str. 2-4
D-60054 Frankfurt/M.

Abstract:

Beside the standard HOM couplers attached on both sides of each cavity the TESLA HOM-damping scheme foresees a broadband absorber that replaces a part of the beam pipe between two sections consisting of eight cavities in a cryostat. To estimate the power that can be expected being deposited in the broadband absorber one has to determine the characteristics of HOM energy propagation through the chain of cavities connected with beam pipes and/or bellows. Therefore a method is presented that allows the broadband measurement of the S-parameters of a single cavity and - using them - the calculation of the behaviour of a N-cavity chain. Up to now the method is restricted to the first (TE_{11}-) waveguide mode.

Introduction:

The beam quality in a linear collider may be affected due to HOMs. Therefore one has to look for fields with high shunt impedance (esp. TM-type), poor coupling to the standard HOM-couplers and low transmission through the cavity channel (i.e. poor coupling to the absorbers between the cryomodules).

Preliminary numerical simulations with MAFIA of a beam pipe part connected to a nine cell cavity showed field distributions located only in the cavity, only in the beam pipe and also in both parts coupled strongly to each other. There seems to be no easy rule that allows a prediction of that cavity-beam pipe-coupling for a given frequency. Therefore a method is needed allowing to determine this coupling experimentally. It appears that the procedure described in this paper can furthermore provide information about the energy dissipation in the standard HOM couplers.

S-parameters describe the reflection of an incoming rf signal at the ports of a certain device and the transmission through the device from one port to the other. They can be arranged to a matrix representation that enables determination of the behaviour of a chain of elements by a simple matrix multiplication of the individual matrix of each element. Therefore they are useful quantities for the study of energy propagation through a channel of cavities by determination of the properties of a single cavity (assuming identical cavities).

The measurement of S-parameters can be easily performed with network analyzers. The major difficulty is caused by the transmission line standard used to connect the cavities to each other: From the rf point of view the beam pipe is a hollow waveguide of circular cross section, in contrast to the coaxial transmission line that is used for the connection with the network analyzer. Therefore transitions are needed to determine the S-parameters of the cavity with respect to their reference plane at the mounting flanges. These transitions (as well as the necessary cabling to the network analyzer and the analyzers ports itself) have own frequency dependend S-parameters that have to be eliminated from the direct measurement results. That means, this environment has to be calibrated.

Such a calibration (or sometimes called: de-embedding problem) is a standard procedure. Normally one uses a set of standards, containing a short, an open and a broadband match to calibrate a single port adaptor. Again, the special difficulty arises from the circular waveguides. Using them, it appears to be very difficult to have a broadband match that is sufficient for calibration purposes. Therefore one has to choose standards which can be built with the necessary precision. It turnes out that this condition leads to the so-called TSD calibration scheme, that uses a Through, a Short and a Delay line. Although the method is decribed in the literature [1, 2] we will explain the mathematical derivation. The method is not very popular due to its sensitivity to connection errors [3]. Since in our case the connections are comparably large flanges that are fixed with several srews, from our experience this problem seemed to be less serious.

The Calibration Procedure:

To measure the S-parameters of the cavity one has to study the following setup:

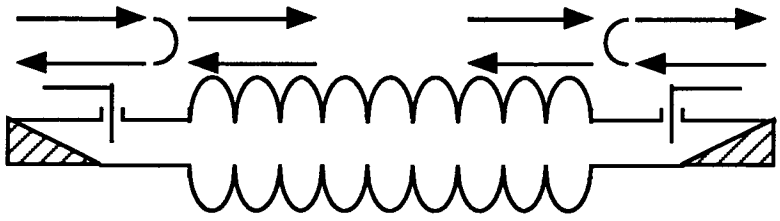

The arrows indicate the signal flow direction from and to the network analyzer. The adaptors are equiped with absorbing materials (hatched triangles) to avoid resonances in the coupling system as far as possible. There is *no need* of a match.
This system contains three unknown parts:

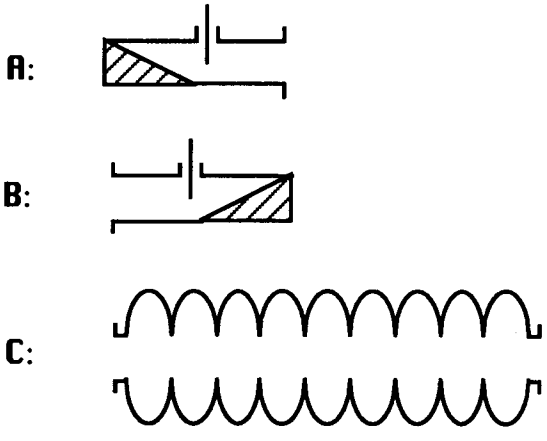

A, **B** and **C** describe the cascadable representation of the S-parameters of both adaptors and the cavity resp. in the following way:

$$\mathbf{S} = \frac{1}{S_{12}} \begin{pmatrix} S_0 & S_{11} \\ -S_{22} & 1 \end{pmatrix} \quad \text{with} \quad S_0 = S_{21} \cdot S_{12} - S_{11} \cdot S_{22} \,, \tag{1}$$

which allows the description of a chain of elements by matrix multiplication (S_{11}, S_{22}: reflection at port 1, port 2; S_{21}, S_{12}: transmission from port 1 to port 2, vice versa).
All objects under discussion fulfill the reciprocity criterion:

$$S_{21} = S_{12} \tag{2}$$

The following quantities can be measured:

Through: $\mathbf{E} = \mathbf{A} \cdot \mathbf{B}$ (3)

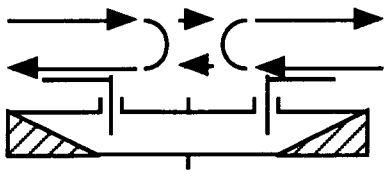

Delay: $\mathbf{F} = \mathbf{A} \cdot \mathbf{D} \cdot \mathbf{B}$ (4)

Short: $\Gamma = \frac{A_{11} - A_0}{1 + A_{22}}$ (5)

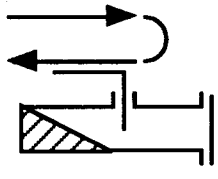

It is not necessary to perform a measurement with port B shortened at the waveguide, but one can use this additional information later for the purpose of controlling the results of calibration.

Solving (3) for $\mathbf{B}$, one gets:

$$\mathbf{B} = \mathbf{A}^{-1} \cdot \mathbf{E} \tag{6}$$

and with (4):

$$\mathbf{F} = \mathbf{A} \cdot \mathbf{D} \cdot \mathbf{A}^{-1} \cdot \mathbf{E} \tag{7}$$

Introducing as abbreviation $\mathbf{T}$

$$\mathbf{F} \cdot \mathbf{E}^{-1} = \mathbf{T}, \tag{8}$$

that depends only on measured quantities, one achieves:

$$\mathbf{T} \cdot \mathbf{A} = \mathbf{A} \cdot \mathbf{D} \tag{9}$$

$\mathbf{D}$ describes the calibration line, that is assumed to be matched at both ports. Its propagation constant γ and length L may be unknown; only the following form of the matrix is important:

$$\mathbf{D} = \begin{pmatrix} e^{\gamma L} & 0 \\ 0 & e^{-\gamma L} \end{pmatrix} \tag{10}$$

Using (10) the evaluation of (9)

$$\frac{1}{T_{12}}\begin{pmatrix} T_0 & T_{11} \\ -T_{22} & 1 \end{pmatrix}\frac{1}{A_{12}}\begin{pmatrix} A_0 & A_{11} \\ -A_{22} & 1 \end{pmatrix} = \frac{1}{A_{12}}\begin{pmatrix} A_0 & A_{11} \\ -A_{22} & 1 \end{pmatrix}\begin{pmatrix} e^{\gamma L} & 0 \\ 0 & e^{-\gamma L} \end{pmatrix}$$

leads to a set of four equations:

$$\begin{aligned}
\frac{1}{T_{12}}(T_0A_0 - T_{11}A_{22}) &= A_0e^{\gamma L} \\
\frac{1}{T_{12}}(T_0A_{11} + T_{11}) &= A_{11}e^{-\gamma L} \\
\frac{1}{T_{12}}(T_{22}A_0 + A_{22}) &= A_{22}e^{\gamma L} \\
\frac{1}{T_{12}}(-T_{22}A_{11} + 1) &= e^{-\gamma L}
\end{aligned} \tag{11 a-d}$$

This can be written in the form of a homogeneous 4x4 - system:

$$\begin{pmatrix} (T_0 - T_{12}e^{\gamma L}) & -T_{11} & 0 & 0 \\ 0 & 0 & (T_0 - T_{12}e^{-\gamma L}) & T_{11} \\ T_{22} & (1 - T_{12}e^{\gamma L}) & 0 & 0 \\ 0 & 0 & -T_{22} & (1 - T_{12}e^{-\gamma L}) \end{pmatrix}\begin{pmatrix} A_0 \\ A_{22} \\ A_{11} \\ 1 \end{pmatrix} = 0 \tag{12}$$

A nontrivial solution exists only in the case of a vanishing determinant of the 4x4 - matrix. Then the second and third line of the matrix can be exchanged so that the problem splits into two sub-determinants with the same characteristic polynom in $e^{\pm\gamma L}$:

$$e^{\pm 2\gamma L} - \frac{T_0 + 1}{T_{12}}e^{\pm\gamma L} + \frac{(T_0 + T_{11}T_{22})}{(T_{12})^2} = 0 \tag{13}$$

With the definition of T_0

$$T_0 = T_{12}\,T_{21} - T_{11}\,T_{22}$$

and the reciprocity (2) the third term can be simplified to 1; furthermore holds:

$$\mathrm{tr}(\mathbf{T}) = \mathrm{tr}\left(\frac{1}{T_{12}}\begin{pmatrix} T_0 & T_{11} \\ -T_{22} & 1 \end{pmatrix}\right) = \frac{T_0 + 1}{T_{12}} \tag{14}$$

Finally dividing (13) by $e^{\pm\gamma L}$ one achieves:

$$\mathrm{tr}(\mathbf{T}) = e^{\pm\gamma L} + e^{\mp\gamma L} = 2\cosh(\pm\gamma L) \tag{15}$$

or solved for $\pm\gamma L$:

$$\pm\gamma L = \operatorname{arccosh}\left(\frac{\mathrm{tr}(\mathbf{T})}{2}\right) . \tag{16}$$

It has to be emphasized that γL (or taking into account the ambiguities of sign and $n\cdot 2\pi$ the expression

$$\pm\gamma L + i\cdot n\cdot 2\pi \;)$$

is a result of the calibration and needs not to be initially known.
Manipulating (11 a,b) (first equations) or (11 c,d) (second equations) one gets two expressions of similar shape for A_{11} and $(-A_0/A_{22})$ with the additional quantities z_1, z_2:

$$\left\{ \begin{array}{l} A_{11} = z_1 \\ -\dfrac{A_0}{A_{22}} = z_2 \end{array} \right\} = \left\{ \begin{array}{l} \dfrac{T_{11}}{T_{12}\, e^{-\gamma L} - T_0} = \dfrac{1 - T_{12}\, e^{-\gamma L}}{T_{22}} \\ \dfrac{T_{11}}{T_{12}\, e^{\gamma L} - T_0} = \dfrac{1 - T_{12}\, e^{\gamma L}}{T_{22}} \end{array} \right\} \tag{17 a,b}$$

Because of the ambiguity of sign in (16) the expressions on the left hand side may be exchanged; this decision will be taken later.
With (5) one has sufficient information to determine from

$$A_{11} = z_1 \; , \quad -\frac{A_0}{A_{22}} = z_2 \; , \quad \frac{A_{11} - A_0}{1 + A_{22}} = \Gamma \tag{18 a-c}$$

A_0 and A_{22}:

$$A_0 = z_2 \frac{\Gamma - z_1}{\Gamma - z_2}$$

$$A_{22} = \frac{z_1 - \Gamma}{\Gamma - z_2} \tag{19 a,b}$$

The calculation from (17) to (19) has to be done in parallel for both cases; each leading to a solution $\mathbf{A}_1$, $\mathbf{A}_2$ for $\mathbf{A}$. Equation (9) is tested with both solutions, now using the phase advance γL_{theo}, that can be calculated from length and diameter of the calibration line and the frequency:

$$\mathbf{T}\cdot\mathbf{A}_{1,2} = \mathbf{A}_{1,2}\cdot\mathbf{D}_{theo}$$

This test is more or less the comparison of the phase advances resulting from the calibration with the value expected from the dimensions of the line. Normally, one solution fits very good whereas the second one doesn't. Difficulties arise only in the neighbourhood of

$$\gamma L = i \cdot \frac{2\pi}{\lambda} L = i \cdot n \cdot \pi \quad \Rightarrow \quad L_{crit.} = \frac{n}{2} \lambda \tag{20}$$

Then follows $e^{+\gamma L} = e^{-\gamma L} = \pm 1$ and consequently with

$$\mathbf{D} = \begin{pmatrix} \pm 1 & 0 \\ 0 & \pm 1 \end{pmatrix}$$

from (7):

$$\mathbf{F} = \mathbf{A} \cdot \mathbf{D} \cdot \mathbf{A}^{-1} \cdot \mathbf{E} = \pm \mathbf{A} \cdot \mathbf{A}^{-1} \cdot \mathbf{E} = \pm \mathbf{E}$$

Then the delay-line measurement contributes no information so that the calibration problem cannot be solved. In the neighbourhood of (20) the errors become very large so that this range has to be avoided (e.g. by using two different delays).
Fig. 1 shows an illustrative example of a reflection factor of one port as a result of two calibration procedures with different line length.

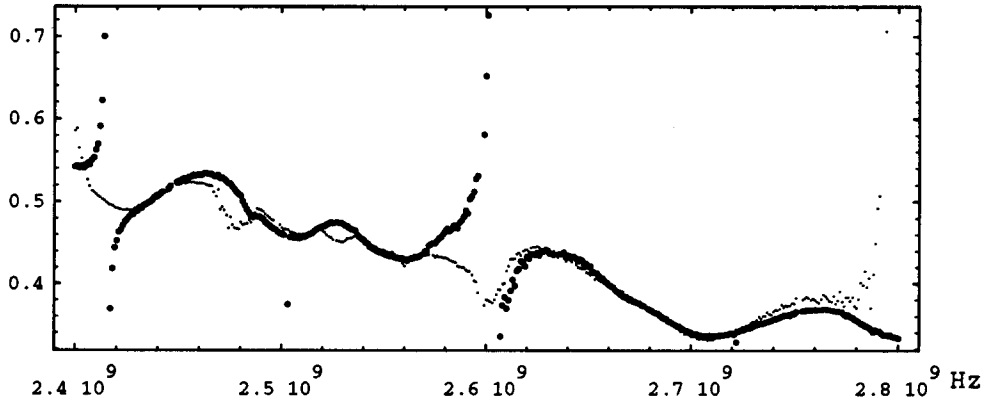

Fig. 1: Waveguide input reflection factor of port A (old), measured with delay lines of 343 mm (bold dots) and 90.1 mm length. Near the $n/2 \cdot \lambda$–points (found by theory at 2.41 and 2.61 GHz (343 mm) and 2.80 GHz (90.1 mm)) a second line is needed to calibrate.

After calibrating port A $\mathbf{B}$ and the cavity properties $\mathbf{C}$ are extracted from

$$\mathbf{B} = \mathbf{A}^{-1} \cdot \mathbf{E} \,, \quad \mathbf{C} = \mathbf{A}^{-1} \cdot \mathbf{G} \cdot \mathbf{B}^{-1} \tag{21}$$

with $\mathbf{G}$ the measurement results of the complete setup.

Measurement Results:

The following series of pictures shows the result of the calibration of a set of two adaptors. The phase information is in all cases also available, but not displayed.
The adaptors (compare fig. 2)

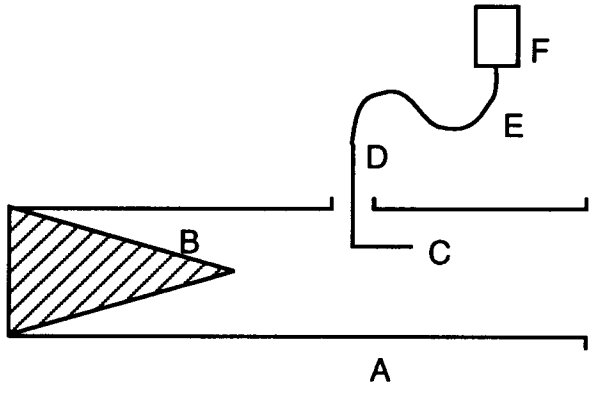

Fig. 2 Schematic cut through one adaptor. (Compare the text for the meaning of the labels.)

consist of a shortened circular waveguide part (A) with a cone of absorbing material (B) inserted. The purpose of this cone is to avoid reflections and therefore resonances as far as possible, but there is no need of a perfect match. The antenna (C) is formed to couple both to TE- and TM-type modes. The connection (D) to the coaxial cable (E), this cable itself and the input port (F) of the network analyzer belong to the adaptor and are calibrated, too.
The following measurements have been performed:

Adaptor A - Adaptor B Adaptor A - Delay 90.1 mm - Adaptor B Adaptor A - Short	Calibration
Adaptor B - Short	Control
Adaptor A - Cavity 1 - Adaptor B Adaptor A - Cavity 2 - Adaptor B Adaptor A - Cavity 1 - Delay 343 mm - Cavity 2 - Adaptor B	Cavity

All measurements cover the same frequency range from 2.4 GHz to 2.64 GHz, using 401 evenly distributed points. The cavities have not been equiped with the standard-HOM-dampers.

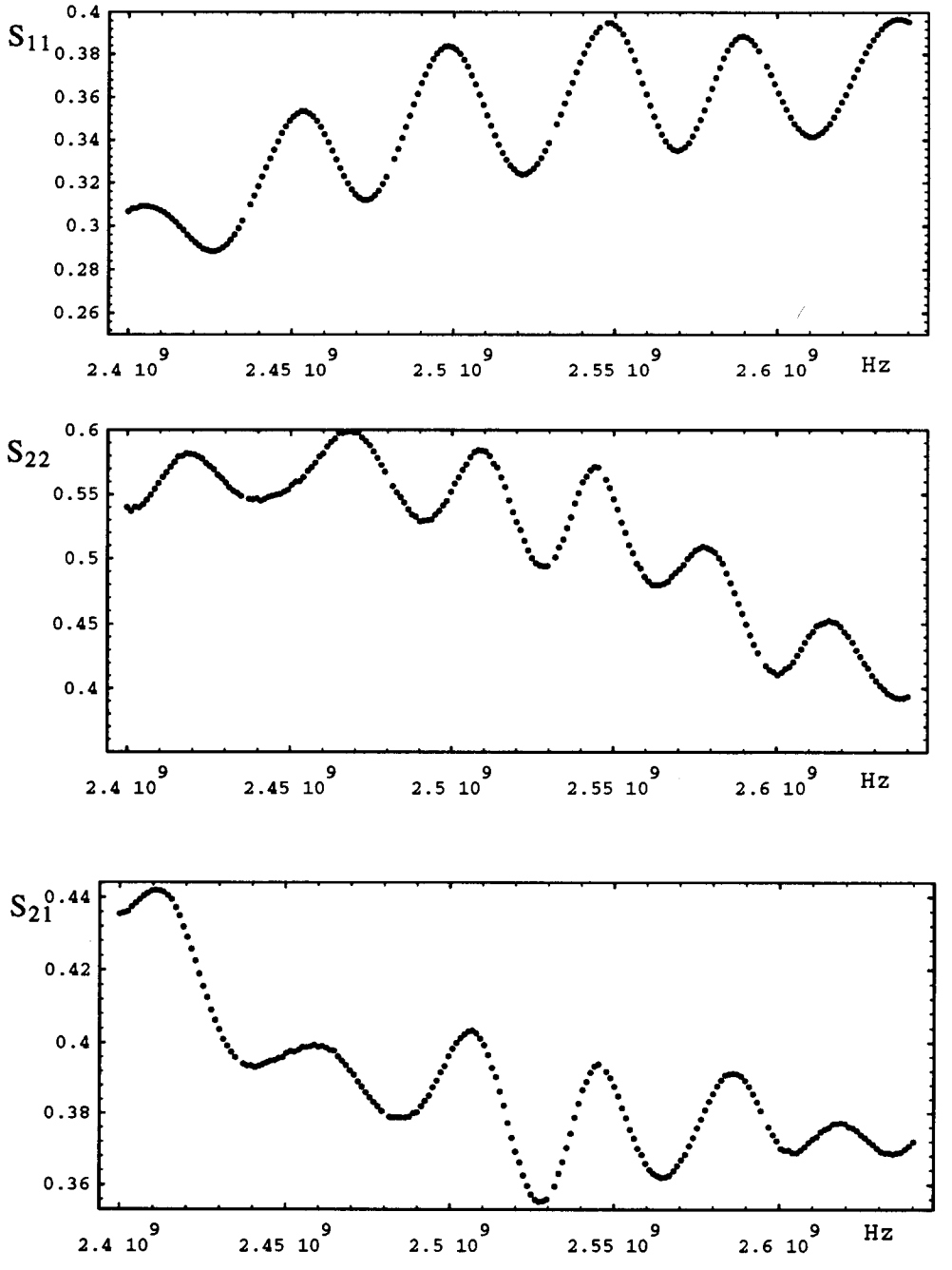

Fig. 3: Calibration results of port A from 2.4 GHz to 2.64 GHz: S_{11} (reflection coaxial), S_{22} (reflection waveguide), S_{21} (transmission)

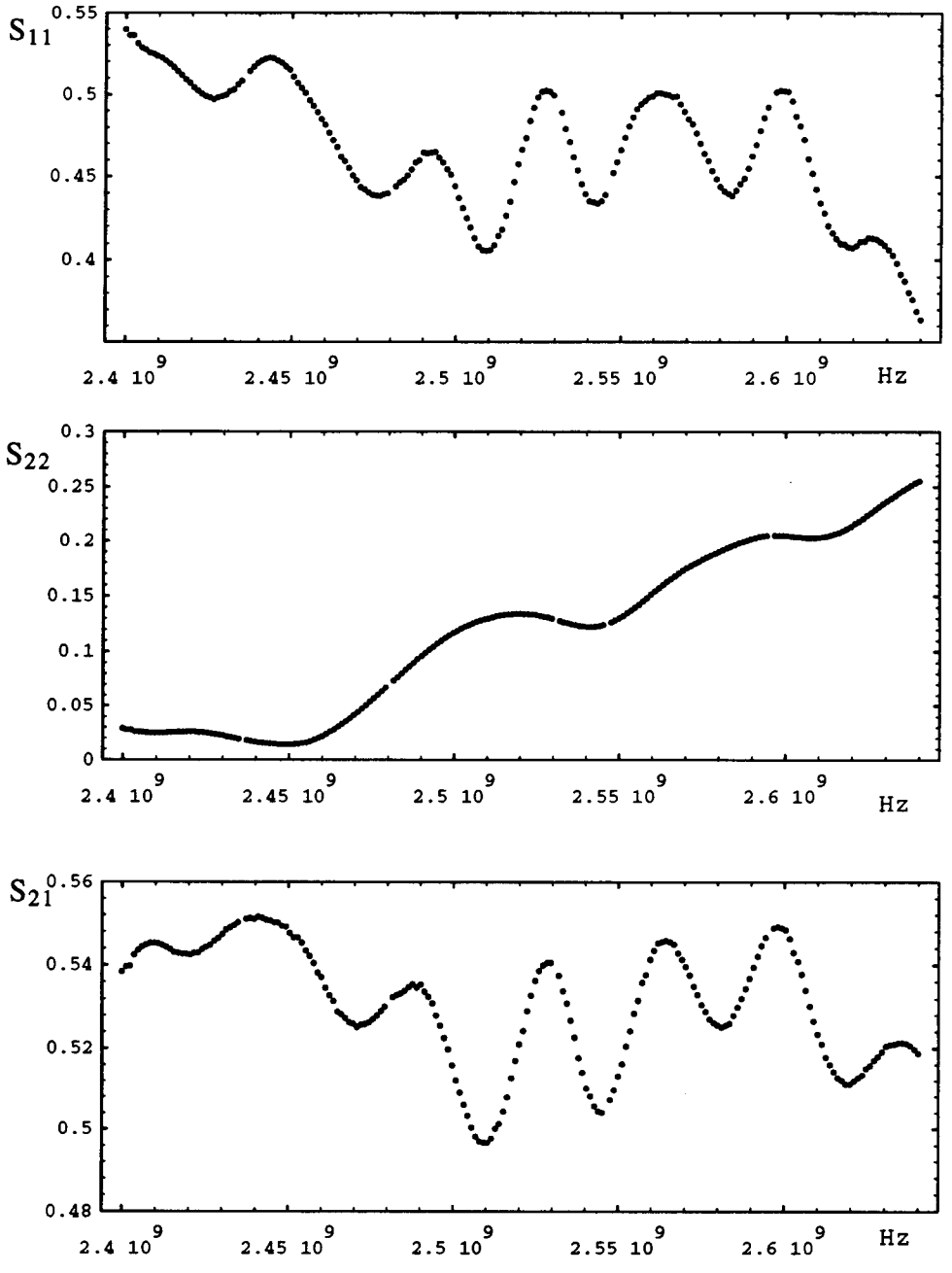

Fig. 4: Calibration results of port B: S_{11} (reflection waveguide), S_{22} (reflection coaxial), S_{21} (transmission)

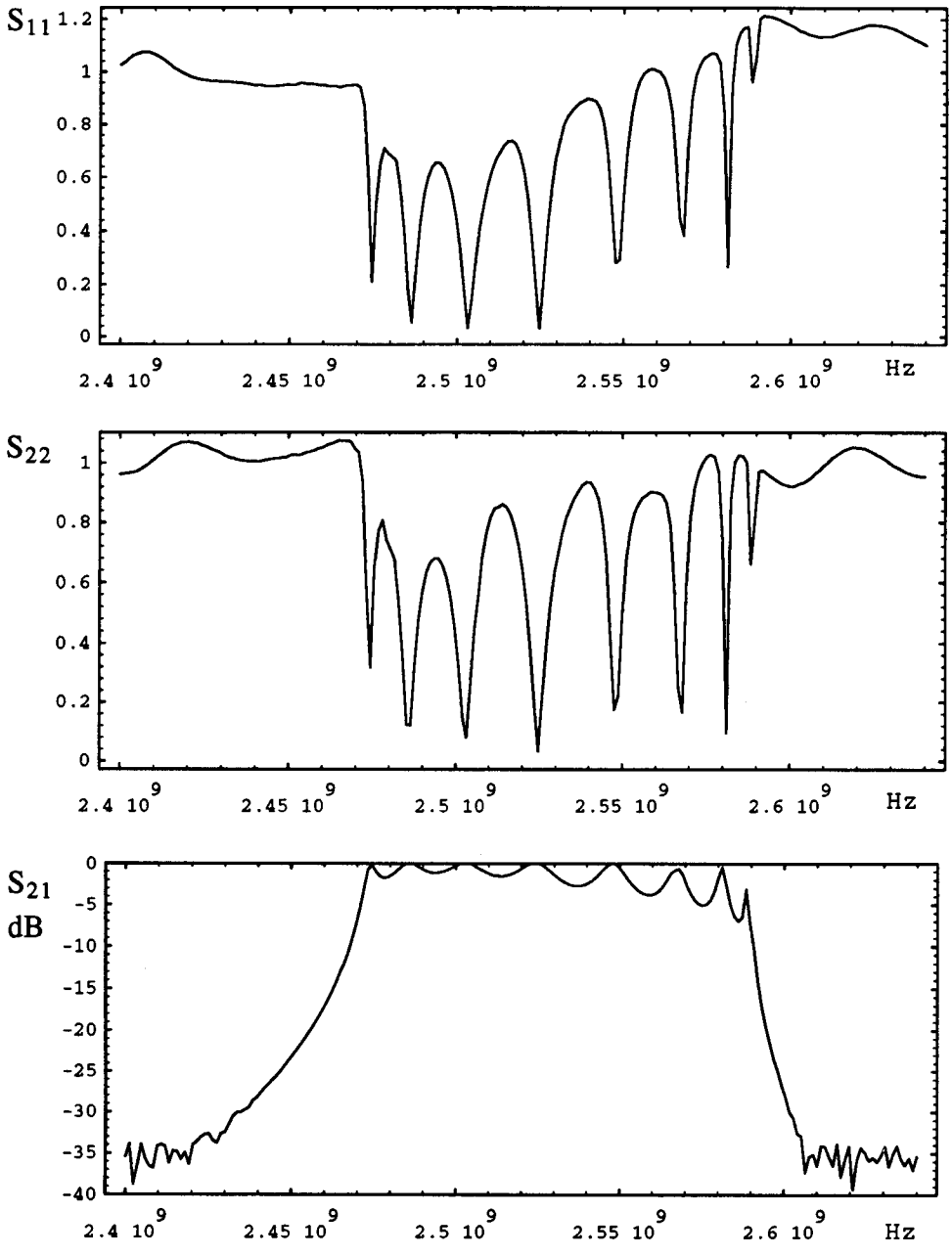

Fig. 5: Measurement results of cavity 1: S_{11}, S_{22} (reflection waveguide); S_{21} (transmission) Obviously the appearance of reflection factors above 1 is due to errors. It is not clear yet, whether this errors are caused by limited reproduceability of the waveguide connections or a consequence of the precision limits of the network analyzer.

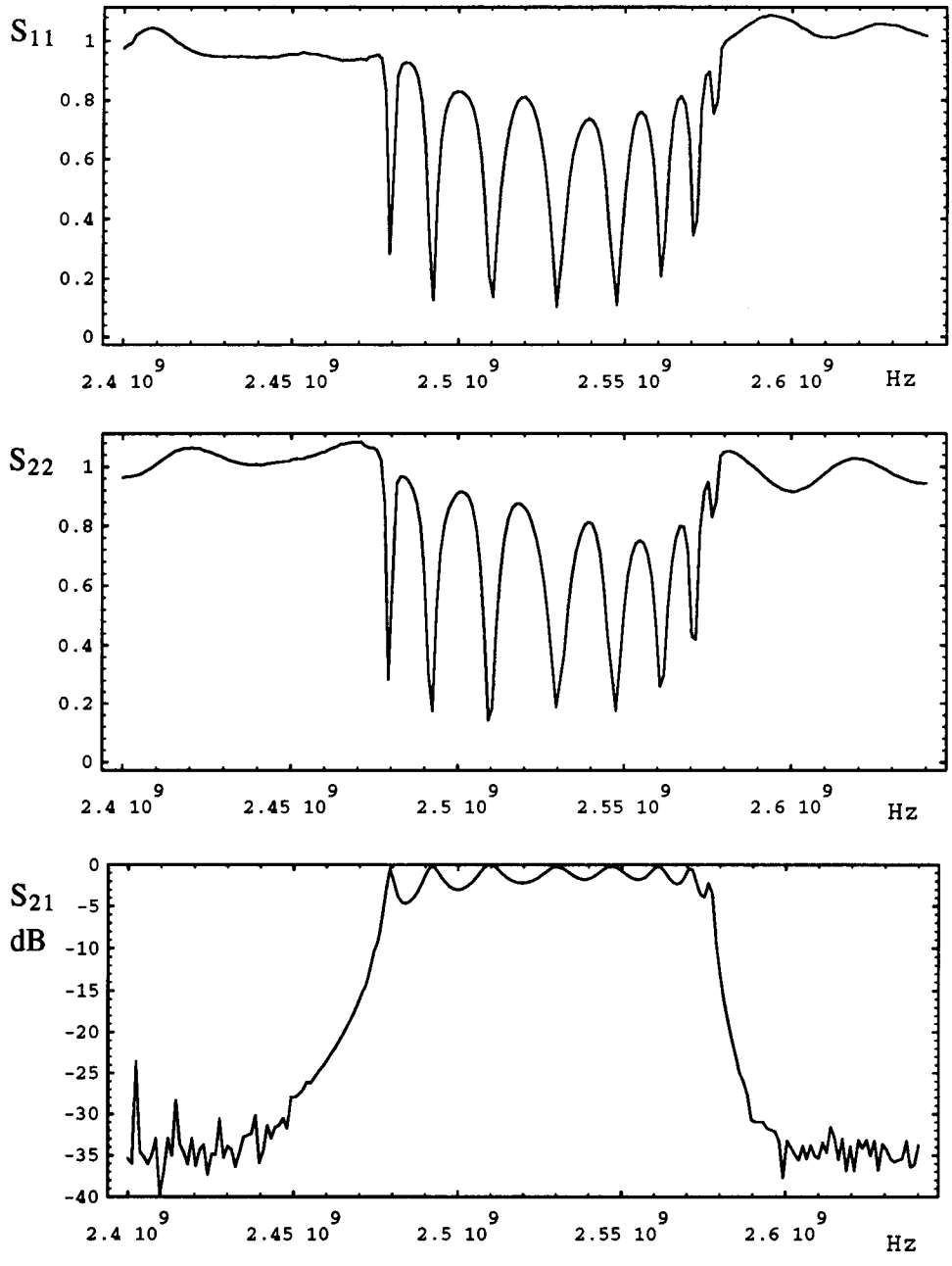

Fig. 6 Measurement results of cavity 2: S_{11}, S_{22} (reflection waveguide); S_{21} (transmission) In spite of the quite similar view of the cavities the measurements allow a distinction between both cavities.

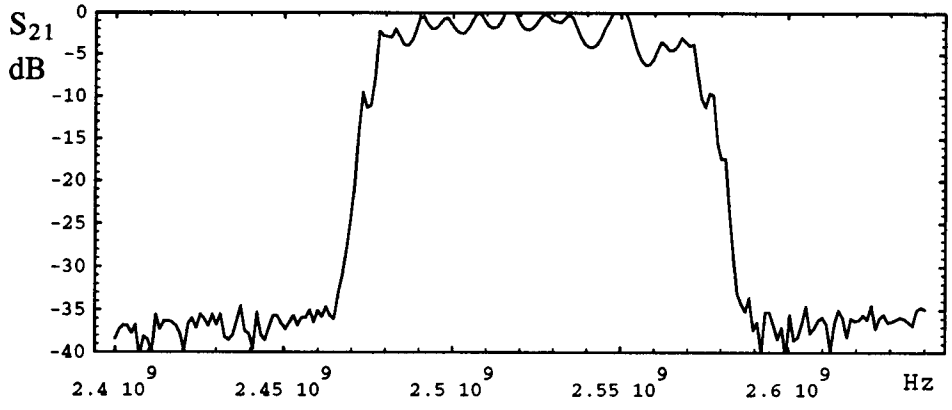

Fig. 7 Value of the transmission through a chain consisting of cavity 1 and 2, connected with a beam pipe of 343 mm length, calculated from single cell measurements

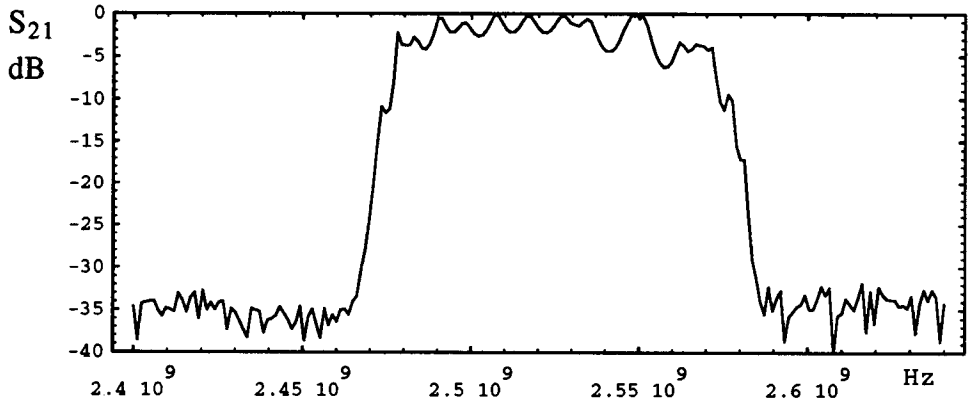

Fig. 8 Measured value of the transmission through a chain consisting of cavity 1 and 2, connected with a beam pipe of 343 mm length

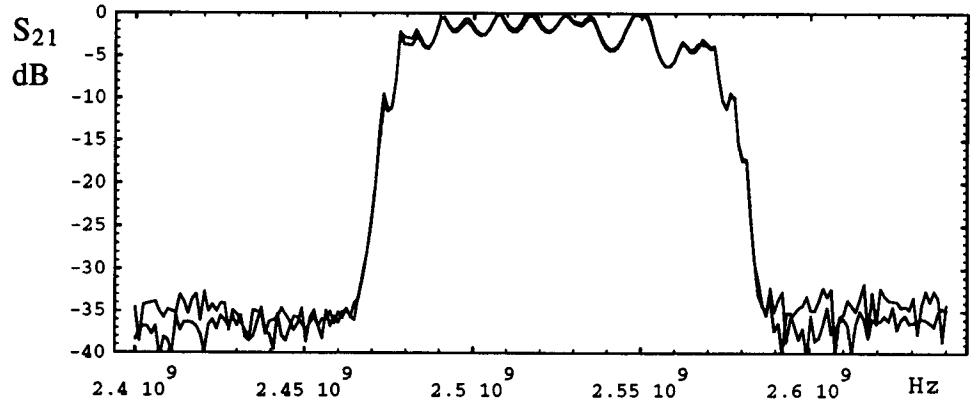

Fig. 9 Both curves of fig. 7 and fig. 8 displayed in one diagramm. In spite of the errors mentioned above, calculation and measurement match quite well.

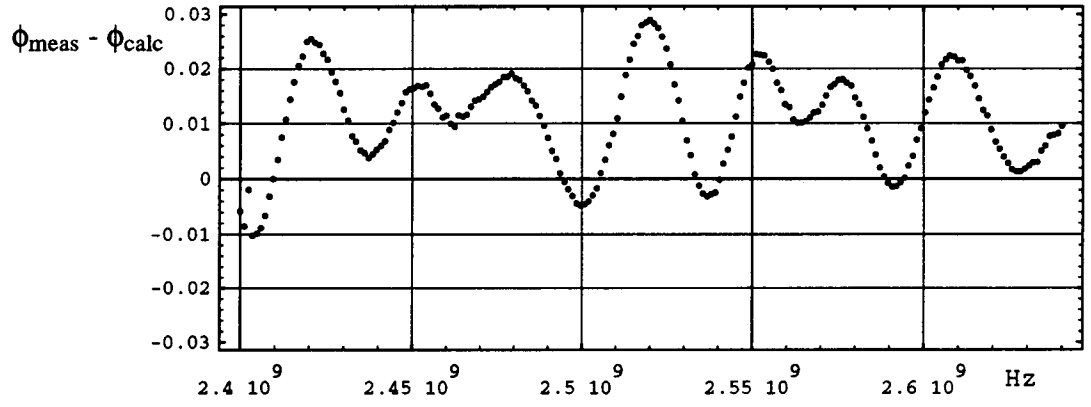

Fig. 10 Difference of the calibration lines phase constant measured during the calibration (compare eq. (16)) and calculated from length, diameter and frequency. Variations are below ≈2°.

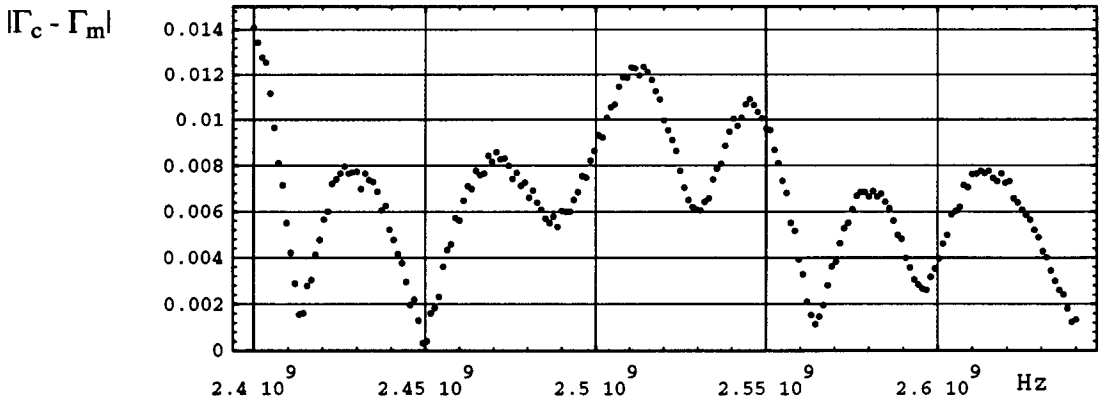

Fig. 11 Comparison of the input reflection factors of port B, being shortened at the waveguide port. Displayed is the difference of Γ_C, calculated from the S-parameters found from the calibration, and Γ_m, measured directly.

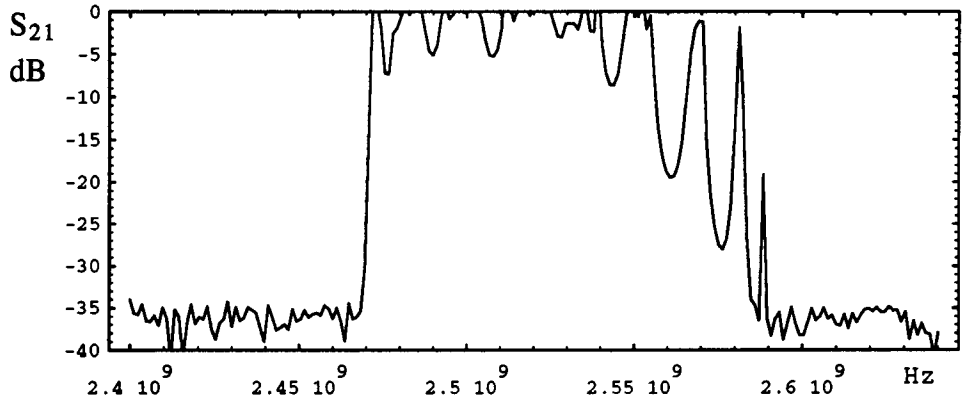

Fig. 12 Calculated value of the transmission through a chain consisting of four identical cavities with the properties of cavity 2, connected with beam pipes of 343 mm length.
One can observe the typical behaviour of a chain of identical filters, i.e. all slopes getting higher with an increasing number of chain elements.

Conclusion:

A method has been presented that allows the determination of the reflection and transmission behaviour of a cavity (or any other device in such an environment, e.g. HOM-damper) with respect to its waveguide ports. Using this data one is able to predict the properties of a chain of devices of arbitrary length (fig. 12).

The reason for the errors causing reflection factors above 1 is unknown. The mistakes due to mounting and dismantling of the waveguide connections are difficult to estimate and may differ extremly each time. The inherent controls of the method (fig. 10, 11) and the comparison of measured and calculated transmission of a two-cavity-chain (fig. 9) show sufficient precision.

Up to now, the method is restricted to the frequency range in which only the first waveguide mode is able to propagate (in the case of 78 mm diameter from 2.25 GHz to 2.95 GHz). With the appearance of additional modes one needs an (quadratically) increasing number of S-parameters to characterize any device independent on the incident mode mix. Therefore the calibration becomes much more complicated.

To get an idea of the typical behaviour in the multimode regime and to identify transmission gaps, that are most severe with respect to HOM-damping, uncalibrated cavity measurements have been performed. These will be reported in a further paper.

References:

[1] G.F. Engen, C.A. Hoer: "Thru-Reflect-Line": An Improved Technique for Calibrating the Dual Six-Port Automatic Network Analyzer, IEEE-Trans.-MTT 27, 12 (Dec. 79), pp. 987

[2] R. Pantoja et.al.: Improved Calibration and Measurement of the Scattering Parameters of Microwave Integrated Circuits, IEEE-Trans.-MTT 37, 11 (Nov. 89), pp. 1675

[3] K. Kindler: Streifenleitungs-Kalibrierung automatischer Netzwerk-Analysatoren mit der TSD-Methode, Archiv der elektrischen Übertragung (AEÜ) 42, 4 (1988), pp. 262